Int J Adv Manuf Technol (2006) 28: 1089–1096
DOI 10.1007/s00170-004-2459-y

ORIGINAL ARTICLE

Zhong-Yi Cai · Ming-Zhe Li · Xi-Di Chen

Digitized die forming system for sheet metal and springback minimizing technique

Received: 25 September 2004 / Accepted: 27 October 2004 / Published online: 22 June 2005

Abstract A flexible production system for sheet metal parts was developed based on the "digitized die" concept. The system can produce a variety of three-dimensional parts without the need for conventional dies, and given only the geometry and the material information of the desired part. The digitized die forming (DDF) system includes the forming press, the shape control system, and software modules with the functions of forming process planning, digitized die shape design, forming process numerical simulation, and springback correction. The digitized die installed in the forming press is the kernel component of the system, it is composed of a pair of matrices of punches, and sheet metal is formed by the enveloping surface of the punches. The working surface of the digitized die are modeled by Non-Uniform Rational B-Spline (NURBS) and constructed by adjusting the height of each punch. Forming process simulation software was developed based on updated Lagrangian formulation and elastic-plastic material model of the finite element, it conducts the numerical simulation to predict the springback and forming defect that may occur in the forming process. A simulation-based approach to compensate for material springback was developed, by correcting the forming surface numerically, an accurate digitized die surface for desired part is obtained. In this paper, the overall structure of the DDF system and the methods of design and control of digitized die shape are described, the detailed steps of the die shape correction for springback and forming process simulation are explained. Applications of the system for the forming of typical sheet metal parts are described.

Keywords Flexible forming · Multi-point forming · Numerical simulation · Sheet metal · Springback

Notation

$B_{i,k}(u)$, $B_{j,l}(v)$: The normalized B-spline base functions
$\boldsymbol{C}^{(k)}$: The correcting matrix for the working surface

Z.-Y. Cai (✉) · M.-Z. Li · X.-D. Chen
Roll Forging Research Institute,
Jilin University,
5988 Renmin Street, Changchun, 130025, P.R. China
E-mail: czy@jlu.edu.cn

$E_S^{(k)}$:	The total shape error of deformed part
h :	The thickness of sheet metal
J_Γ :	Jacobian determinant
k :	The number of correcting iteration
k_T, k_N :	Penalty coefficients in the tangential and normal direction
$\boldsymbol{k}_\mathrm{c}$:	The stiffness matrix of the contact element
$\boldsymbol{K}_\mathrm{T}$:	Tangent stiffness matrix
$\boldsymbol{K}_\mathrm{C}$:	Contact stiffness matrix
$\boldsymbol{n}$:	The normal vector of the surface
$\boldsymbol{N}$:	Shape function matrix of finite element
$\boldsymbol{p}(u, v)$:	Objective shape of desired part
$\boldsymbol{P}_{i,j}$:	The control points of NURBS surface
$\boldsymbol{p}_c^U$, $\boldsymbol{p}_c^L$:	The position vector of the center of upper and lower punch spheric end
$\boldsymbol{P}$:	Array of the heights of punches (represents the shape of the working surface)
$\boldsymbol{P}^{(k)}$:	The shape of the working surface after k-correcting iteration
r :	The radii of punch spheric end
${}^t\boldsymbol{R}_\mathrm{ce}$, ${}^{t+\Delta t}\boldsymbol{R}_\mathrm{ce}$:	The vectors of external nodal contact forces at time t and $t+\Delta t$
${}^t\boldsymbol{R}_\mathrm{ci}$:	The vector of internal contact forces at time t
${}^t\boldsymbol{R}_\mathrm{ext}$, ${}^{t+\Delta t}\boldsymbol{R}_\mathrm{ext}$:	The vectors of prescribed external nodal forces at time t and $t+\Delta t$
${}^t\boldsymbol{R}_{int}$:	The vector of the internal nodal forces at time t
$\boldsymbol{S}$:	Array of the z-coordinates of the surface of formed part at sampling points
$\boldsymbol{S}_\mathrm{obj}$:	The objective shape of desired part
$\boldsymbol{t}_T$:	The tangential component of the contact forces
$\boldsymbol{T}$:	The transformation matrix between local coordinate and global coordinate
$\omega_{i,j}$:	The corresponding weights of $\boldsymbol{P}_{i,j}$
$\Delta\boldsymbol{P}$:	The increment of the working surface
$\Delta\boldsymbol{R}$:	Load increment vector
$\Delta\boldsymbol{S}$:	The shape error of the formed part
$\Delta\boldsymbol{S}^{(k)}$:	The shape error of the formed part after k-correcting iteration
$\Delta\boldsymbol{U}$:	Displacement increment vector

μ : Friction coefficient
α : Contact state factor

1 Introduction

A sheet metal part is usually formed with dies, manufactured in accordance with the shape and dimensions of the part. The die design process is an iterative procedure of trail and error, it results in considerable lead times and costs in the production of the dies. This conventional method is adequate for mass production because the cost of dies can be shared by a large number of products. Recently, however, flexible die and dieless forming methods for a small size lot are being developed, since the customer's demand is so diversified that the lot size has become small.

Among various techniques for a small size lot, the idea of a forming die of variable shape has gained great attention since it would permit the design iterations to be rapid and nearly cost free. Iwasaki, Shiota, and Taura [1] developed a triple-row-press to form simple three-dimensional sheet metal parts. Hardt, Boyce, and Walczky [2–5] explored the mechanical design and shape control algorithms of discrete die tooling, the developmental technology known as reconfigurable tooling for flexible fabrication (RTFF). They developed a reconfigurable tool that replaced multiple dies employed in stretch-forming sheet metal aircraft components. Li and co-workers [6–16] have made a series of progress on the so-called "multi-point forming (MPF) method for sheet metal" [6, 7]. As the working surface of die can be constructed in real-time, a sheet part can be manufactured along a specific forming path in MPF [10–12]. When the path of deformation is designed properly, forming defects will be avoided completely and lager deformation is achieved. A sheet metal part can be formed section by section through the sectional MPF [14, 15], and this technique makes it possible to manufacture large size parts in a small MPF press.

The "digitized die forming (DDF)" concept is derived from MPF. The conventional stamping dies are replaced by a pair of matrices of punches with hemispheric ends, by controlling the height of each punch, the matrix of punches is approximately a continues working surface of the die. A digitized die photograph is shown in Fig. 1. The working volume of the die is $400 \times 320 \times 100$ mm, the punches tips can form any arbitrary surface that can be contained in the working volume. With finer punches and smaller space between punches, a better surface approximation is realized, and higher quality products can be achieved in DDF.

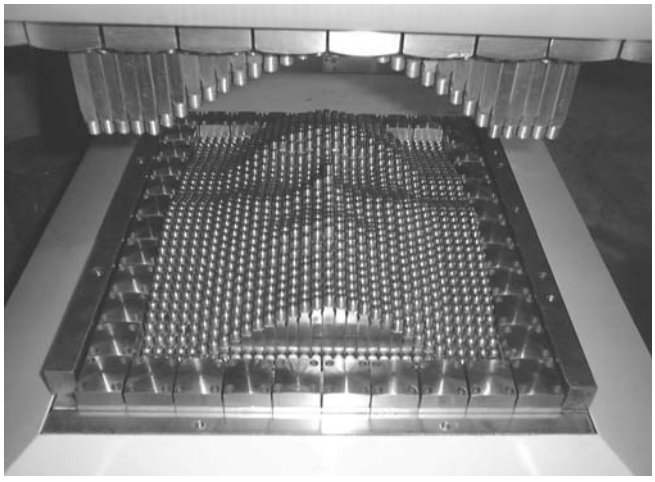

Fig. 1. A digitized-die, 40×32 punches constructing a 400 mm $\times$ 320 mm working area

The DDF system would permit the design of a forming die to be rapid and nearly cost free when making new parts. The availability of an easily variable shape of digitized die can be used to compensate for springback or other production variables.

2 Forming system

A typical DDF system is composed of three parts: DDF press, software system, and computer control system. The digitized die installed in the DDF press is the kernel component of the system, and the computer control system command DDF press to adjust the height of punch to establish the working surface of the digitized die and to control the DDF press to apply the forming loads. The software system is comprised by the following modules: module for planning of forming process, module of digitized die design, module for forming process simulation and forming defects prediction, and module for springback correction. Figure 2 shows the overall process for digitized die shape design and sheet metal forming. The top layer of Fig. 2 shows the information flow, the middle layer shows the sequence of activ-

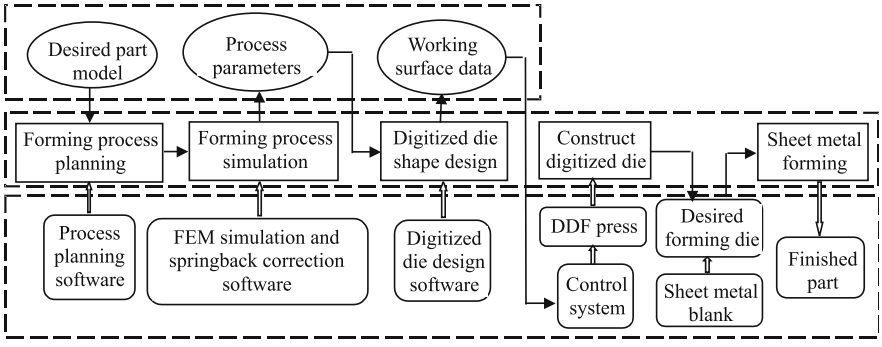

Fig. 2. Sheet metal forming process by DDF system

ities, and the bottom layer depicts the basic components in the DDF system.

All activities in the forming process are realized through corresponding software. The process planning software designs DDF procedures and determines process parameters based on the information of the sheet metal part to be formed. Finite Element Analysis (FEA) software simulates the DDF process numerically and predicts the defects that may occur in the forming process then determines the optimal technological parameters. Springback correction software is developed on the basis of numerical simulation, an iterative procedure is employed to correct the shape of the digitized die, and minimize springback finally. Digitized die design software computes the height of each punch and determines the process parameters, displays the constructing process of digitized die virtually, and checks the punch distances of travel as well as the contact state between punches and the virtual part. If any punch interferes with the objective shape of to be formed, it is necessary to return to the planning step and revise the DDF process. An effective solution is to adopt the sectional DDF technique, which can realize large deformation by forming sheet blank in a section-by-section way [14].

3 Design of the digitized die shape

3.1 Calculation of working surface

The working surface of the digitized die is the enveloping surface of the spheric end of the punch matrix. The principal work to design the digitized die shape is to determine the position coordinates in the height direction of the spheric end of every punch.

In Fig. 3, the equation of the objective shape for a desired part is $\boldsymbol{p} = \boldsymbol{p}(u, v)$, if expressed by the NURBS surface with control points $\boldsymbol{P}_{i,j} (0 \le i \le n, 0 \le j \le m)$, it can be defined as:

$$\boldsymbol{p}(u, v) = \frac{\sum_{j=0}^{n}\sum_{i=0}^{m} \omega_{j,i}\boldsymbol{P}_{j,i}B_{i,k}(u)B_{j,l}(v)}{\sum_{j=0}^{n}\sum_{i=0}^{m} \omega_{j,i}B_{i,k}(u)B_{j,l}(v)} \quad (u_{k-1} \le u \le u_{n+1}, v_{l-1} \le v \le v_{m+1}) \tag{1}$$

where $\omega_{i,j}$ are the corresponding weights of $\boldsymbol{P}_{i,j}$, $B_{i,k}(u)$ and $B_{j,l}(v)$ are the normalized B-spline base functions of order k and l, respectively, defined over knot vector $\boldsymbol{u} = \{u_0, u_1, \cdots, u_n, \cdots, u_{n+k}\}^{\mathrm{T}}$ and $\boldsymbol{v} = \{v_0, v_1, \cdots, v_m, \cdots, v_{m+l}\}^{\mathrm{T}}$.

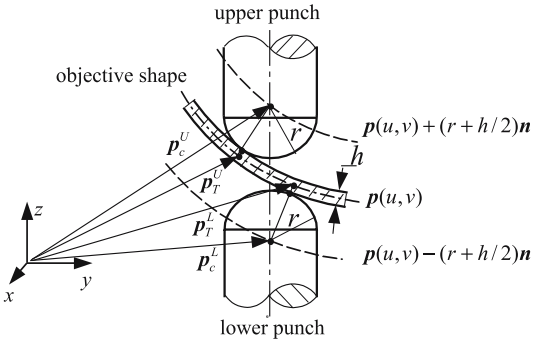

Fig. 3. Calculation of the height of punch in digitized die

The position coordinates of the centers of an upper and a lower punch spheric end can be calculated from the following equations:

$$\begin{cases} \boldsymbol{p}(u, v) + (r + h/2)\boldsymbol{n} = \boldsymbol{p}_c^U \\ \boldsymbol{p}(u, v) - (r + h/2)\boldsymbol{n} = \boldsymbol{p}_c^L \end{cases} \tag{2}$$

where $\boldsymbol{p}_c^U = (x_c^U, y_c^U, z_c^U)^{\mathrm{T}}$ and $\boldsymbol{p}_c^L = (x_c^L, y_c^L, z_c^L)^{\mathrm{T}}$ are the position vector of the center of the upper and lower punch spheric end, respectively, r is the radii of the punch spheric end, h is the thickness of sheet metal, and $\boldsymbol{n}$ is the normal vector of surface $\boldsymbol{p}(u, v)$, and is written as:

$$\boldsymbol{n}(u, v) = \frac{\boldsymbol{p}_u(u, v) \times \boldsymbol{p}_v(u, v)}{|\boldsymbol{p}_u(u, v) \times \boldsymbol{p}_v(u, v)|}. \tag{3}$$

The tangential vector can be derived from Eq. 1:

$$\begin{cases} \boldsymbol{p}_u(u, v) = [\boldsymbol{P'}_u(u, v) - w_u(u, v)\boldsymbol{p}(u, v)]/w(u, v) \\ \boldsymbol{p}_v(u, v) = [\boldsymbol{P'}_v(u, v) - w_v(u, v)\boldsymbol{p}(u, v)]/w(u, v) \end{cases} \tag{4}$$

where

$$\boldsymbol{P'}_u(u, v) = \sum_{j=0}^{n}\sum_{i=0}^{m} \omega_{j,i}\boldsymbol{P}_{j,i}\dot{B}_{i,k}(u)B_{j,l}(v),$$

$$\boldsymbol{P'}_v(u, v) = \sum_{j=0}^{n}\sum_{i=0}^{m} \omega_{j,i}\boldsymbol{P}_{j,i}B_{i,k}(u)\dot{B}_{j,l}(v),$$

$$w(u, v) = \sum_{j=0}^{n}\sum_{i=0}^{m} \omega_{j,i}B_{i,k}(u)B_{j,l}(v),$$

$$w_u(u, v) = \sum_{j=0}^{n}\sum_{i=0}^{m} \omega_{j,i}\dot{B}_{i,k}(u)B_{j,l}(v),$$

$$w_v(u, v) = \sum_{j=0}^{n}\sum_{i=0}^{m} \omega_{j,i}B_{i,k}(u)\dot{B}_{j,l}(v).$$

3.2 Digital die shape control

Each punch in the digitized die is supported on a lead screw. According to the data of a designed working surface, the computer control system commands motors to actuate the screw and adjust the height of each punch then establish the desired die shape. Two strategies – serial mode and parallel mode, for controlling the die shape have been developed [15].

The serial mode is a slow but inexpensive way to change the digitized die configuration, it is realized based on a manipulator. Figure 4 shows an adjusting process of the serial mode for a digitized die configuration. The manipulator moves on the x and y-axis and adjusts a single punch at a time (as the shaded punch shown in Fig. 4). It therefore takes a long time to finish a desired die shape and the more punches the digitized die contains, the longer time it will take.

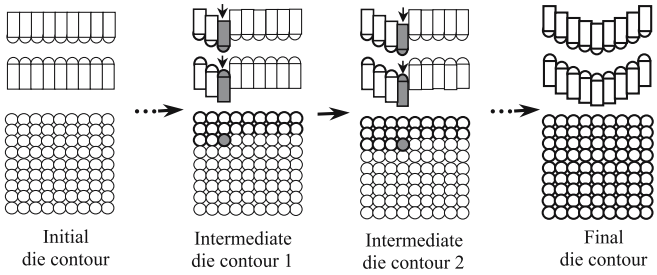

Fig. 4. Sketch of the serial mode for controlling digitized die shape

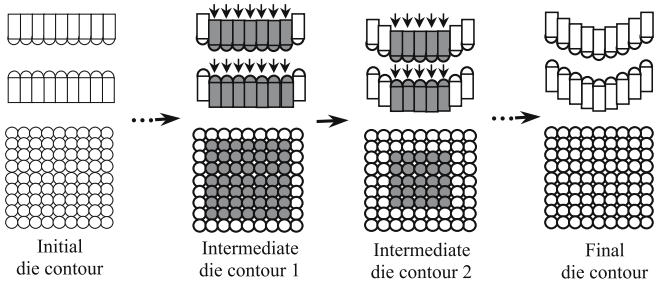

Fig. 5. Sketch of the parallel mode for controlling digitized die shape

Figure 5 shows an adjusting process of the parallel mode for a digitized die configuration. In this mode, each punch is controlled by a so-called "Computerized Numerical Control (CNC) unit", and each unit contains a microprocessor board, a mini-motor, and a set of driving gears. The board consists of a microprocessor, motor controller chips, and associated circuitry. Computer-controlled motors move the punches along their axes individually and all punches are adjusted simultaneously. Parallel mode is a rapid way to change die shape, the setup time for a given forming surface is depend on the largest variation of height among all punches, and it is independent of the number of punches.

4 Springback correction

The springback will occur after removing the applied loads from the deformed sheet, resulting in the deviation of the formed part from the applied die shape, and springback must be considered during the design of the sheet metal process. It is necessary to compensate for springback by shape change of the die surface. To determine the amount of shape change during the forming process, a quantitative prediction of springback is very important. A numerical simulation-based technique to minimize springback on the digitized die was developed. A user-friendly software system has been created. The system can predicts the proper die shape to obtain perfectly shaped parts and therefore eliminate the need for any forming trials or iterations.

4.1 Forming process simulation

In order to obtain the correct stress status in the finite element analysis of forming process, then achieve high accuracy of the amount of springback, a software for the simulation of DDF was developed based on updated Lagrangian formulation and elastic-plastic material model of finite element. The finite element formulations have been described in detail in reference [11, 16], and receives only a brief outline here.

Starting from a deformed state of equilibrium at time t, the sheet blank is thus loaded by a load increment $\Delta \boldsymbol{R}$, causing an additional displacement and deformation $\Delta \boldsymbol{U}$ which is defined by the equilibrium condition for the new configuration at $t+\Delta t$. The approximate linear equation for $\Delta \boldsymbol{U}$ can be written as:

$$(\boldsymbol{K}_{\mathrm{T}}+\boldsymbol{K}_{\mathrm{C}})\Delta \boldsymbol{U} = {}^{t+\Delta t}\boldsymbol{R}_{\mathrm{ext}} + {}^{t+\Delta t}\boldsymbol{R}_{\mathrm{ce}} - {}^{t}\boldsymbol{R}_{\mathrm{int}} - {}^{t}\boldsymbol{R}_{\mathrm{ci}} \tag{5}$$

where $\boldsymbol{K}_{\mathrm{T}} = \frac{\partial {}^{t}\boldsymbol{R}_{int}}{\partial \boldsymbol{U}}$, $\boldsymbol{K}_{\mathrm{C}} = \frac{\partial {}^{t}\boldsymbol{R}_{\mathrm{ci}}}{\partial \boldsymbol{U}}$, ${}^{t+\Delta t}\boldsymbol{R}_{\mathrm{ext}} = {}^{t}\boldsymbol{R}_{\mathrm{ext}} + \Delta {}^{t}\boldsymbol{R}_{\mathrm{ext}}$, ${}^{t+\Delta t}\boldsymbol{R}_{\mathrm{ce}} = {}^{t}\boldsymbol{R}_{\mathrm{ce}} + \Delta {}^{t}\boldsymbol{R}_{\mathrm{ce}}$; ${}^{t}\boldsymbol{R}_{int}$ is the vector of the internal nodal forces due to stress at time t. ${}^{t}\boldsymbol{R}_{\mathrm{ext}}$, ${}^{t+\Delta t}\boldsymbol{R}_{\mathrm{ext}}$ are the vectors of prescribed external nodal forces at time t and $t+\Delta t$, respectively, ${}^{t}\boldsymbol{R}_{\mathrm{ci}}$ is the vector of internal contact forces at time t and ${}^{t}\boldsymbol{R}_{\mathrm{ce}}$, ${}^{t+\Delta t}\boldsymbol{R}_{\mathrm{ce}}$ are the vectors of external nodal contact forces at time t and $t+\Delta t$, respectively.

In DDF, the contact area is multi-point and discontinuous, its behavior is more complicated than that in conventional stamp forming. The treatment of contact interface is one of the most important issues in the simulation of a DDF process. An incremental analysis procedure is the demanded, and effective constraint methods are required so that the contact condition on the contact boundaries may be imposed. Interface behavior of frictional contact is formulated by the penalty method and Coulomb non-classical friction law. The three-dimensional contact element is adopted to model the multi-point contact surface and the highly nonlinear contact problem is treated in an incremental way.

Covering contact boundary with a layer of contact element and interpolating the penetrations at the contact point by finite element formulation, a symmetric stiffness matrix for a contact element can be deduced [11, 16]:

$$\boldsymbol{k}_{\mathrm{c}} = \int_{\Gamma_{\mathrm{c}}} \boldsymbol{N}^{\mathrm{T}}\, \boldsymbol{T}\boldsymbol{E}_{\mathrm{c}T}\, \boldsymbol{T}^{\mathrm{T}}\, \boldsymbol{N} J_{\Gamma}\, \mathrm{d}\xi\, \mathrm{d}\eta \tag{6}$$

where Γ_{c} is defined as the contact boundary on which the sheet is in or being in contact with digitized die, $\boldsymbol{N}$ is the shape function matrix, $\boldsymbol{T}$ is the orthogonal transformation matrix between the local coordinate and global coordinate at the contact point, J_{Γ} is the Jacobian determinant of the local coordinate $\xi-\eta$. Also, the incremental form of frictional contact constitutive matrix is given by:

$$\boldsymbol{E}_{cT} = \begin{bmatrix} k_T\left(1-\alpha\frac{t_{T1}^2}{|\boldsymbol{t}_T|^2}\right) & -\alpha k_T \frac{t_{T1}t_{T2}}{|\boldsymbol{t}_T|^2} & \alpha\mu k_N \frac{t_{T1}}{|\boldsymbol{t}_T|} \\ -\alpha k_T \frac{t_{T1}t_{T2}}{|\boldsymbol{t}_T|^2} & k_T\left(1-\alpha\frac{t_{T2}^2}{|\boldsymbol{t}_T|^2}\right) & \alpha\mu k_N \frac{t_{T2}}{|\boldsymbol{t}_T|} \\ 0 & 0 & k_N \end{bmatrix} \tag{7}$$

where $\boldsymbol{t}_T = (t_{T1}t_{T2})^{\mathrm{T}}$ is the tangential component of the contact forces and k_T, k_N penalty coefficients in tangential and normal direction, μ is the friction coefficient, and α is a factor of the

contact state. In the sticking contact state, $\alpha = 0$, and if sliding contact occurs, $\alpha = 1$.

After assembling the contact stiffness into the global stiffness matrix, we obtain the final finite equations. In this method the stiffness matrix is still positive definite [16], finite element equations do not contain additional variables and can be solved by the approaches used in ordinary finite element analysis.

Figure 6 schematically depicts the sequential procedure of that which was utilized in the forming process simulation. Briefly, the elastic-plastic material model of the finite element was used to analyze the forming process in which a deformable blank was brought into contact with a pair of rigid forming dies, and the entire external load was applied in a number of increments and the corresponding nonlinear equations were solved though an equilibrium iterating procedure. At the completion of the loading process, the deformed shape, stresses, and strains within the elements were transferred into the portion of the program for unloading process analysis. This was accomplished by creating a database file that updated the geometry and stress history of element.

Once in the unloading process, the die components were removed from the model, forming pressure was transferred to external load, and valid boundary conditions were applied to the deformed blank to restrain rigid body motion. Then the forming pressure was removed incrementally and the Newton–Raphson iterative procedure was utilized in each incremental step to determine the subsequent springback deformations in the deformed blank that occurred after removal from dies.

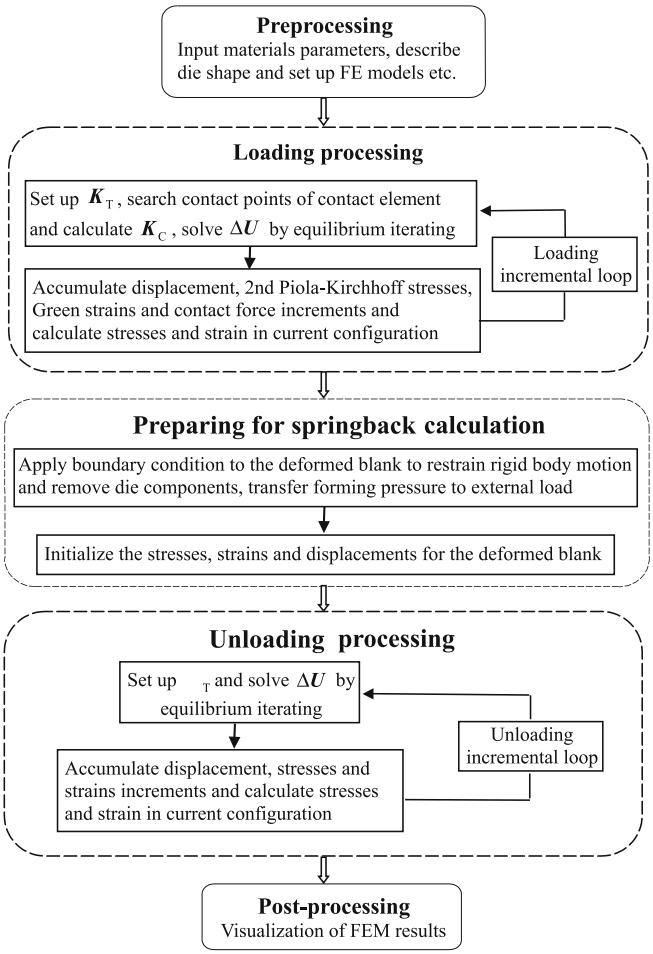

Fig. 6. Sequential procedure of DDF process simulation

4.2 Die shape corrections for springback

For a digitized die comprised by $m \times n$ punches on each side, the surface of a deformed blank can be expressed as a function of the heights of all punches $p_i (i = 1, 2, \cdots, m \times n)$:

$$S(x, y) = f(p_1, p_2, \cdots, p_{mn}) . \tag{8}$$

If surface $S(x, y)$ is represented by $m \times n$ discrete points, Eq. 5 is then written by the following equation

$$\boldsymbol{S} = \boldsymbol{F}(\boldsymbol{P}) \tag{9}$$

where $\boldsymbol{S} = \{S_1 S_2 \cdots S_{mn}\}^{\mathrm{T}}$ is an $m \times n$ array of the z-coordinates of discrete sampling points, it represents the shape of the deformed part. $\boldsymbol{P} = \{p_1 p_2 \cdots p_{mn}\}^{\mathrm{T}}$ is an $m \times n$ array of the heights of punches, it represents the working surface of the digitized die corresponding to surface $\boldsymbol{S}$; $\boldsymbol{F} = \{F_1 F_2 \cdots F_{mn}\}^{\mathrm{T}}$ and $S_i = F_i(p_1, p_2, \cdots, p_{mn})$.

From Eq. 6, the increment of the working surface $\Delta \boldsymbol{P}$ can be calculated approximately from the increment of the shape of the deformed blank $\Delta \boldsymbol{S}$ as follow:

$$\Delta \boldsymbol{P} = \boldsymbol{C} \Delta \boldsymbol{S} \tag{10}$$

where $\boldsymbol{C} = \nabla^{-1} \boldsymbol{F}$ is an $(m \times n) \times (m \times n)$ matrix, and

$$\nabla \boldsymbol{F} = \begin{bmatrix} \partial F_1/\partial p_1 & \partial F_1/\partial p_2 & \cdots \partial F_1/\partial p_{mn} \\ \partial F_2/\partial p_1 & \partial F_2/\partial p_2 & \cdots \partial F_2/\partial p_{mn} \\ \vdots & \vdots & \vdots \ \vdots \\ \partial F_{mn}/\partial p_1 & \partial F_{mn}/\partial p_2 & \cdots \partial F_{mn}/\partial p_{mn} \end{bmatrix} . \tag{11}$$

Let $\boldsymbol{S}_{\mathrm{obj}}$ represents the objective shape of the desired part, and the shape error (as shown in Fig. 7a) of the deformed part is described by

$$\Delta \boldsymbol{S} = \boldsymbol{S}_{\mathrm{obj}} - \boldsymbol{S}. \tag{12}$$

To minimizing springback, the working surface should be corrected step by step based on the shape error of the deformed part. A new working surface can be computed by following the correcting procedure:

$$\boldsymbol{P}^{(k+1)} = \boldsymbol{P}^{(k)} + \boldsymbol{C}^{(k)} \Delta \boldsymbol{S}^{(k)} \tag{13}$$

where k is the number of correcting iteration, $\boldsymbol{P}^{(k)}$ and $\Delta \boldsymbol{S}^{(k)}$ are the shape of the working surface and shape error of the deformed part after k-correcting iteration, respectively, $\boldsymbol{P}^{(k+1)}$ is the working surface for the next iteration (as shown in Fig. 7b), and $\boldsymbol{C}^{(k)} = \nabla^{-1} \boldsymbol{F}^{(k)}$ is a correcting matrix and the element in $\nabla \boldsymbol{F}$

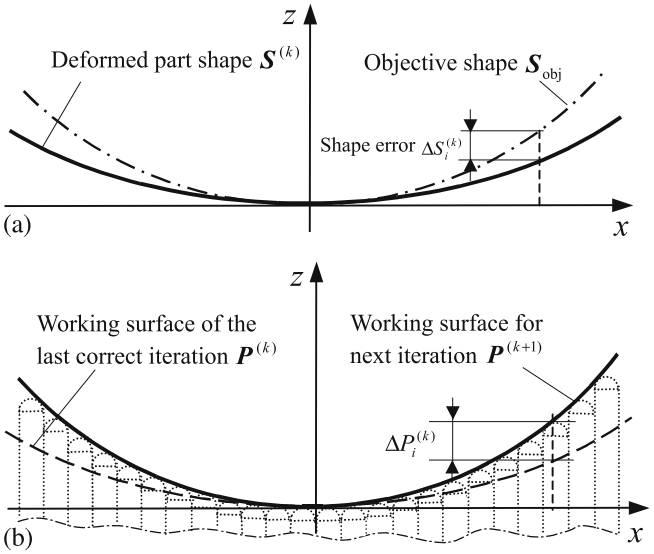

Fig. 7. Springback correcting of the working surface of digitized die

can be calculate approximately based on the results of the last two iterations.

$$\left(\frac{\partial F_i}{\partial P_j}\right)^{(k)} \approx \frac{S_i^{(k)} - S_i^{(k-1)}}{P_j^{(k)} - P_j^{(k-1)}} \tag{14}$$

The total shape error of a deformed part is evaluated by

$$E_S^{(k)} = \frac{1}{mn} \sum_{i=1}^{m \times n} |\Delta S_i^{(k)}|. \tag{15}$$

Figure 8 shows a flowchart of the springback correction process. On the basis of the simulated results of the previous forming cycle, the objective shape of the part is compared to the shape of the deformed part to obtain the shape errors, and these errors are processed to generate a new working surface of the digitized die. This new working surface is then

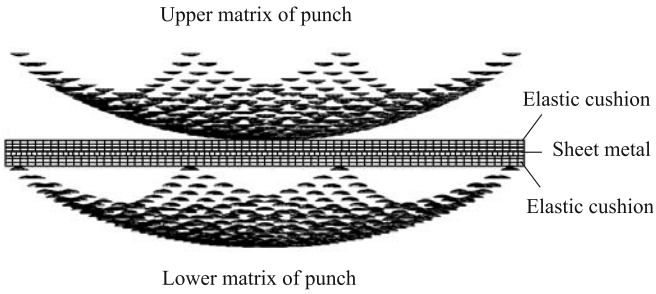

Fig. 9. FEM model for the simulation of DDF process of a spherical objective shape

used to deform the sheet blank and obtain a new deformed part with fewer shape errors. The correcting iteration continues until the prescribed tolerance of the part shape error is satisfied.

4.3 Numerical examples

Based on the developed approach to minimize springback, the die shape correction processes for two typical objective shapes – a cylindrical surface ($R = 200$ mm) and a spherical surface ($R = 1200$ mm), were performed. The digitized die includes 30×30 punches. The initial blanks are square sheets of 300×300 mm, with thickness 1.0, 1.5, and 2.0 mm. The material of the sheets is 08AL with $E = 200.0$ GPa, $v = 0.3$, $n = 0.201$, $K = 537$ MPa, and the initial yield stress $\sigma_y = 128$ MPa. Figure 9 shows a finite element model for the numerical analysis of the DDF process of a spherical surface.

From Eqs. 10 and 11, two forming iterations are required before a new forming surface can be calculated. By setting the working surface to the objective shape of the desired part, that is $P^{(0)} = S_{obj}$, the formed part $S^{(0)}$ was produced and the shape error $\Delta S^{(0)}$ obtained. The first iteration was conduct by taking the correcting matrix as:

$$C^{(1)} = Diag[\rho_1, \rho_2, \cdots, \rho_{mn}] \tag{16}$$

Fig. 8. Die shape correction process for springback based on forming process simulation

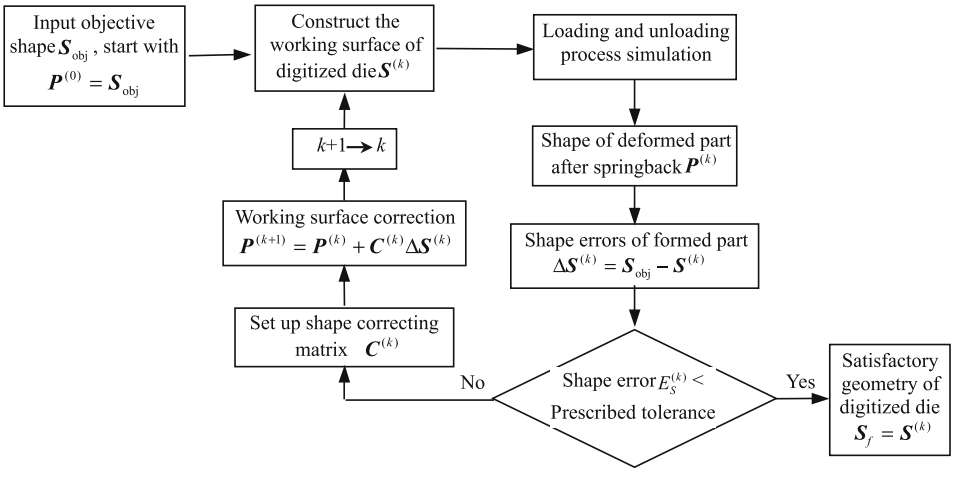

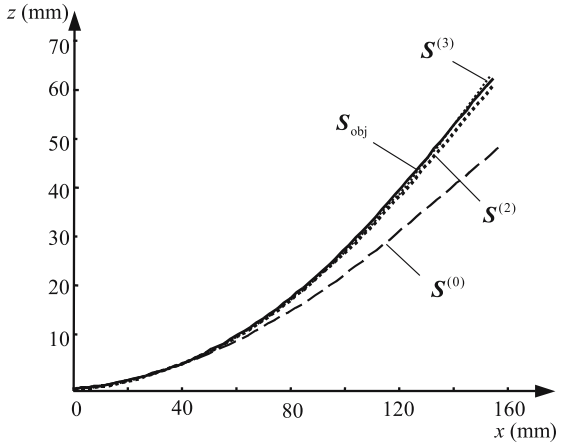

Fig. 10. Variation of the configuration of deformed blank in correcting iteration for a cylindrical objective shape ($R = 200$ mm)

where ρ_i is the curvature of the sampling point i, and $\rho_i = (\rho_{ix} + \rho_{iy})/2$ for a spherical surface. Once these two initial forming iterations are completed, the matrix $\boldsymbol{C}$ can be computed (Eqs. 8 and 11) and the correcting process started. The allowable shape error of 0.05 mm was achieved within four correcting iterations for these two parts. The configuration variation of the deformed blank in the correcting processes for a cylindrical objective shape is shown in Fig. 10, and the shape error and maximum z-coordinate error of each correcting iteration for the objective shapes of cylindrical and spherical surface are listed in Tables 1 and 2, respectively.

Table 1. Shape error and maximum z-coordinate error for a cylindrical objective shape in correcting process for springback

Iteration time k	Thickness of sheet metal h (mm)					
	$h = 1.0$		$h = 1.5$		$h = 2.0$	
	$E_S^{(k)}$ (mm)	ΔS_{max} (mm)	$E_S^{(k)}$ (mm)	ΔS_{max} (mm)	$E_S^{(k)}$ (mm)	ΔS_{max} (mm)
0	0.866	15.57	0.816	12.52	0.318	7.233
1	0.104	3.257	0.206	8.932	0.056	2.094
2	0.087	2.135	0.140	3.671	0.041	0.891
3	0.013	0.371	0.021	0.440	0.011	0.198

Table 2. Shape error and maximum z-coordinate error for a spherical objective shape in correcting process for springback

Iteration time k	Thickness of sheet metal h (mm)			
	$h = 1.5$		$h = 2.0$	
	$E_S^{(k)}$ (mm)	ΔS_{max} (mm)	$E_S^{(k)}$ (mm)	ΔS_{max} (mm)
0	1.411	3.146	1.310	2.783
1	0.251	0.911	0.204	0.573
2	0.096	0.263	0.091	0.211
3	0.033	0.112	0.031	0.105

5 Application of DDF

5.1 Elastic cushion technique

In DDF, punches present concentrated loads to the sheet, and the concentrated loads make the deformations of the sheet strongly localized, dimpling may occur. To suppress dimpling, it is necessary to distribute the loads applied by punches. Extensive experimentation showed that the suppression of dimpling in the sheet metal is easily accomplished by sandwiching the sheet blank between two polymer blankets, the so-called "elastic cushion" technique (as shown in Fig. 11). However, this elastic cushion reduces the resolution of the formed part because it filters out rapid slop changes on the working surface. It is necessary to compensate for the elastic cushion deformation by changing the objective shape of the digitized die surface, the amount of shape change is provided by the FEM simulation.

5.2 DDF with blankholder

During the forming of complex three-dimensional sheet metal parts with large deformation, the in-plane compressive stresses created often lead to failure of wrinkling. In conventional stamping, the wrinkling defect is suppressed by a blankholder which binds the material at the periphery to provide the in-plane tensile bias. In DDF, wrinkling can be eliminated in the same way. A DDF press with a flexible blankholder was developed to manufacture complex sheet metal parts. A schematic of a DDF of sheet metal with a blankholder is shown in Fig. 12. Both upper and lower blankholders are divided into several segments. Each segment is driven by a hydraulic cylinder which is controlled by proportional and servo-valves separately. Thus the blankholder force applied on the blank sheet can be adjusted to meet requirements.

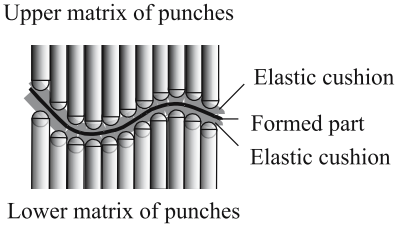

Fig. 11. Digitized-die forming of sheet metal with elastic cushion

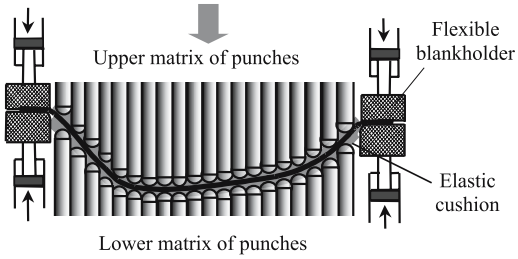

Fig. 12. Digitized-die forming of sheet metal with a blankholder

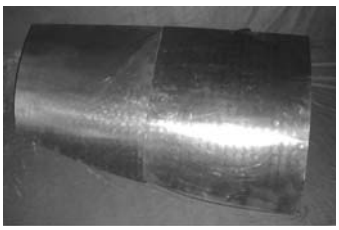
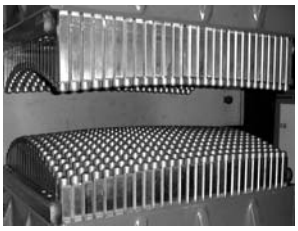

Fig. 13. Sheet metal part formed by digitized-die ($28 \times 20 \times 2$ punches)


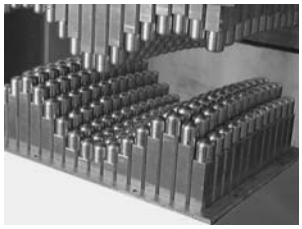

Fig. 14. Sheet metal part formed by digitized-die ($16 \times 12 \times 2$ punches)

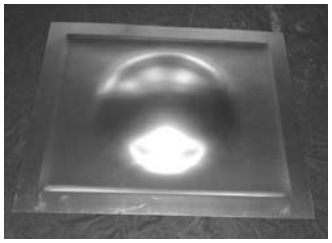
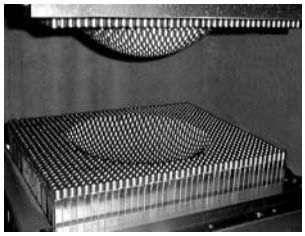

Fig. 15. Sheet metal part formed by digitized-die ($40 \times 32 \times 2$ punches) with blankholder

5.3 Application examples

Up till now, hundreds of sheet metal parts with different shapes and different sizes have been manufactured successfully in the DDF systems we developed. Figures 13 and 14 show two sheet metal parts and the digitized dies that were used to form them. The former digitized die is comprised by 28×20 punches and the later 16×12 punches. Four correcting iterations were performed for these two parts to achieve the die shape that is compensated for the elastic springback of materials.

Figure 15 shows a sheet metal part formed by the digitized die with a blankholder. The die is comprised by 40×32 punches. Experiments showed that without a blankholder in DDF, serious wrinkles arose in the final part, but wrinkles were eliminated completely when a blankholder was adopted.

6 Concluding remarks

Because reconfigurable discrete dies are used in DDF, part manufacturing costs are reduced and manufacturing time is shorten greatly. The DDF system will result in a simpler, more agile, and lower-cost production environment for the manufacturing of sheet metal products. This lean technology could make the manufacturing of sheet metal products more efficient and eliminate the use of a large percentage of the expensive dies that are used now in sheet metal parts construction.

DDF is most suitable for the forming of various shell-like parts. With a blankholder, thin sheet metal parts can be formed without the failure of wrinkling. This technique will be very useful in the manufacturing of complex sheet metal parts such as automobile panels.

Several DDF systems have been developed and they have been applied to different sheet-forming processes including the forming of the skin of high-speed train heads, the forming of ship hull plates, and most recently, the digital forming of titanium prosthesis for the repair of skull defects.

Acknowledgement This work was supported by the National Science Foundation of China (50275063).

References

1. Iwasaki Y, Shiota H, Taura Y (1977) Development of a Triple-row-press. Mitsubishi Heavy Industries, Technical Review
2. Hardt DE, Olsen BA, Allison BT, Pasch K (1981) Sheet metal forming with discrete die surfaces. Proc Ninth American Manufacturing Research Conference, pp 140–144
3. Hardt DE, Webb RD (1982) Sheet metal die forming using closed loop shape control. Ann CIRP 31(1):165–169
4. Hardt DE, Boyce MC, Walczky DF (1993) A flexible forming system for rapid response production of sheet metal parts. Proc IBEC'93, Detroit, MI, USA, pp 61–69
5. Walczyk DF, Hardt DE (1998) Design and analysis of reconfigurable discrete dies for sheet metal forming. J Manuf Syst 17:436–454
6. Li MZ, Nakamura K et al. (1992) Harmful phenomena in multi-point forming (3rd report: Research on multi- point forming for sheet metal). Proc of the 43rd Japanese Joint Conf for Technology of Plasticity, pp 425–428
7. Mingzhe L, Yuhong L et al. (1999) Multi-point forming: a flexible manufacturing method for a 3D surface sheet. J Mater Process Technol 87:277–280
8. Liu CG, Li MZ, Cai ZY (2000) Research on multi-point closed-loop forming of 3D sheet metal parts. China Mech Eng 11(15):1326–1329 (in Chinese)
9. Cai ZY, Li MZ (2001) Optimum path forming technique for sheet metal and its realization in multi-point forming. J Mater Process Technol 110:136–141
10. Cai ZY, Li MZ, Feng ZH (2001) Theory and method of optimum path forming for sheet metal. Chin J Aeronaut 14(2):118–122
11. Cai ZY (2000) Numerical simulation of the forming process and study on the optimum path for multi-point forming of sheet metal. Dissertaion, Jilin University (in Chinese)
12. Cai ZY, Li MZ, Cui XJ (2002) Numerical method for the prediction of net shaped blank in the multi-point forming of sheet metal. Chin J Mech Eng 15(4):314–318
13. Cai ZY, Li MZ (2002) Multi-point forming of three-dimensional sheet metal and the control of the forming process. Int J Press Vessels Piping 79(4):289–296
14. Li MZ, Cai ZY, Sui Z, Yan QG (2002) Multi-point forming technology for sheet metal. J Mater Process Technol 129(1–3):333–338
15. Sui Z, Li MZ, Cai ZY (2002) General design and key technologies research on the control system for multi-point forming. J of Jilin University (Eng and Technol Edn) 32(4):20–24 (in Chinese)
16. Cai ZY, Li MZ (2005) Finite element simulation of Multi-point sheet forming process based on implicit scheme. J Mater Process Technol 161(3):449–455